Liquid chromatographic isolation of individual carbohydrates from environmental matrices for stable carbon analysis and radiocarbon dating

Amel Nouara, Christos Panagiotopoulos, Jérôme Balesdent, Kalliopi Violaki, Edouard Bard, Yoann Fagault, Daniel James Repeta, Richard Sempere

Liquid chromatographic isolation of individual carbohydrates from environmental matrices for stable carbon analysis and radiocarbon dating

Amel Nouara[1], **Christos Panagiotopoulos**[1]***, **Jérôme Balesdent**[2], **Kalliopi Violaki**[1], **Edouard Bard**[2], **Yoann Fagault**[2], **Daniel James Repeta**[3], **Richard Sempéré**[1]

[1]Aix Marseille Univ., Université de Toulon, CNRS, IRD, MIO UM 110, 13288, Marseille, France

[2]Aix Marseille Univ., CNRS, Collège de France, IRD, INRA, CEREGE UM34, 13545 Aix-en-Provence, France

[3]Department of Marine Chemistry and Geochemistry, Woods Hole Oceanographic Institution, Woods Hole, MA 02543, USA

*Corresponding author. Phone: +33 4 86 09 05 26

E-mail : christos.panagiotopoulos@mio.osupytheas.fr

Revised version

February 27, 2019

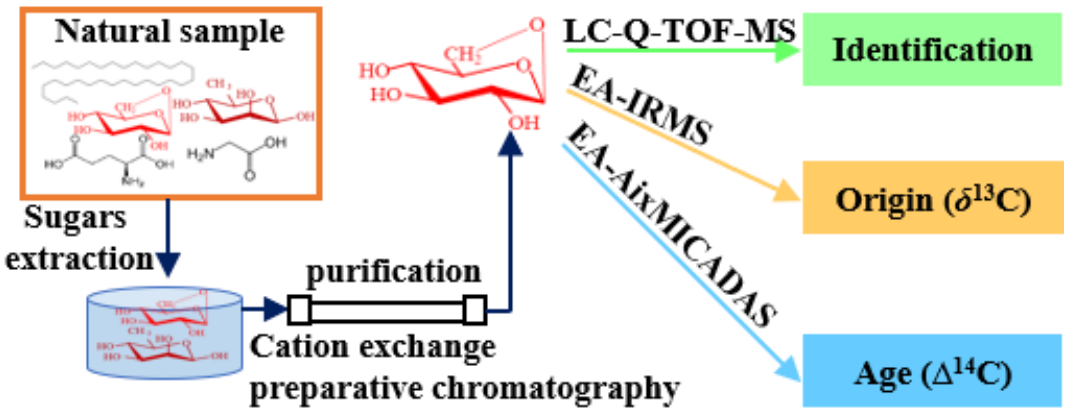

Abstract

Carbohydrates are among the most abundant organic molecules in both aquatic and terrestrial ecosystems; however, very few studies have addressed their isotopic signature using compound-specific isotope analysis, which provides additional information on their origin ($\delta^{13}C$) and fate ($\Delta^{14}C$). In this study, semi-preparative liquid chromatography with refractive index detection (HPLC-RI) was employed to produce pure carbohydrate targets for subsequent offline $\delta^{13}C$ and $\Delta^{14}C$ isotopic analysis. $\delta^{13}C$ analysis was performed by elemental analyzer-isotope ratio mass spectrometer (EA-IRMS) whereas $\Delta^{14}C$ analysis was performed by an innovative measurement procedure based on the direct combustion of the isolated fractions using an elemental analyzer coupled to the gas source of a mini carbon dating system (AixMICADAS). In general, four successive purifications with Na^+, Ca^{2+}, Pb^{2+}, and Ca^{2+} cation-exchange columns were sufficient to produce pure carbohydrates. These carbohydrates were subsequently identified using mass spectrometry by comparing their mass spectra with those of authentic standards.

The applicability of the proposed method was tested on two different environmental samples comprising marine particulate organic matter (POM) and total suspended atmospheric particles (TSP). The obtained results revealed that for the marine POM

sample, the $\delta^{13}C$ values of the individual carbohydrates ranged from −18.5 to −16.8‰, except for levoglucosan and mannosan, which presented values of −27.2 and −26.2‰, respectively. For the TSP sample, the $\delta^{13}C$ values ranged from −26.4 to −25.0‰. The galactose and glucose $\Delta^{14}C$ values were 19 and 43‰, respectively, for the POM sample. On the other hand, the levoglucosan radiocarbon value was 33‰ for the TSP sample. These results suggest that these carbohydrates exhibit a modern age in both of these samples. Radiocarbon HPLC collection window blanks, measured after the addition of phthalic acid (^{14}C free blank), ranged from −988 to −986‰ for the abovementioned compounds, indicating a very small background isotopic influence from the whole purification procedure. Overall, the proposed method does not require derivatization steps, produces extremely low blanks, and may be applied to different types of environmental samples.

Keywords: Semi-preparative liquid chromatography; carbohydrates purification; carbohydrate-specific ^{13}C and ^{14}C analysis; EA-IRMS; EA-AixMICADAS

1. Introduction

Carbohydrates are among the most ubiquitous organic molecules and have been recorded in all geochemical systems, including terrestrial [1,2], marine [3,4], and atmospheric organic matter [5,6]. Although previous investigations have provided a wealth of information on their concentrations and distributions in all geochemical systems [7–11], very less is known about their sources and fate, which have not been thoroughly studied using carbon isotopes. Such information, obtained from carbon

isotope examination at the molecular level, may help trace the origin of the different components of organic matter and explain its reactivity during long-range transport [12].

Bulk carbon isotope analysis generally reflects the average of the isotopic composition of the whole panel of organic molecules inside the sample [13–18]. Further extraction of the sample with acids or organic solvents produces "purified" fractions (e.g. sugar- or lipid-like fractions) and aids in the determination of the isotopic composition of the hydrophilic and hydrophobic components of the sample [18–20]. For example, previous studies on dissolved organic matter (DOM) have reported δ^{13}C values for carbohydrate-like fractions in the ranges −29 to −25‰ in river estuaries [21] and −21.5 to −20.3‰ in the Atlantic and Pacific Oceans [22]. These δ^{13}C values are typical for terrestrial and marine ecosystems, respectively. Moreover, the reported Δ^{14}C values for carbohydrate-like fractions in marine high molecular weight DOM showed a wide range of values spanning from 7 to −406‰, further implying that the age of carbohydrates spans from modern to very old (4180 yr BP) [22]. However, the bulk isotope analysis approach does not completely address the isotopic diversity of the individual molecules inside the sample.

In contrast with bulk isotope analysis, the compound-specific isotope analysis (CSIA) of the individual sugars offers valuable information on the origin (δ^{13}C) and age (Δ^{14}C) of the single molecules [23–27]. The CSIA technique is not a new approach; however, it requires high analytical skills for the purification and extraction of individual molecules from the sample. This step is crucial and might strongly affect the results. The two most commonly employed techniques for the stable carbon isotope analysis of carbohydrates are gas and liquid chromatography coupled with isotope ratio mass spectrometry (GC-IRMS and LC-IRMS, respectively). Since carbohydrates are

not volatile, derivatization steps (silylation or alditol acetate derivatization) are required for GC-IRMS analysis. This further necessitates carbon corrections on the carbohydrate isotopic signatures [23,28–30]. Another disadvantage of the GC-IRMS technique is that two different monosaccharides (e.g. glucose and fructose) can produce the same alditol (e.g. glucitol) during the reduction step of the derivatization procedure, thereby causing a loss of compositional information [31].

LC-IRMS is a good alternative to GC-IRMS because it does not require any derivatization steps [30,32–34]. However, this technique does not target all the sugar components of the sample; for example, neutral sugars, amino sugars, alditols, and anhydrosugars cannot be separated in a single run [35,36]. Moreover, both the GC-IRMS and LC-IRMS techniques cannot be used for $\Delta^{14}C$ determination on single carbohydrates due to their low sensitivity toward the ^{14}C isotope. To date, very few radiocarbon data exist on single carbohydrates comprising neutral sugars, alditols, and anhydrosugars. Alditols and anhydrosugars are important tracers of terrestrial vegetation [37,38] and burning biomass processes [39], respectively. Thus, their isotopic study may help to evaluate their long-range transport from land to sea and more importantly, to assess their reactivity in long time scales (fate) in the marine environment. Although a significant amount of work was done on the compound-specific radiocarbon analysis of individual lipids over the past 20 years [40–43] and more recently, on amino acids [44], a well-established technique for single carbohydrate purification from environmental samples for subsequent radiocarbon measurements has not been reported to date.

An interesting approach to produce pure carbohydrate targets for $\delta^{13}C$ and $\Delta^{14}C$ analysis is the use of semi-preparative high-performance liquid chromatography with refractive index detection (HPLC-RI) on cation-exchange columns. Pure carbohydrates

can be analyzed by an elemental analyzer–isotope ratio mass spectrometer (EA-IRMS) for $\delta^{13}C$ and/or an accelerated mass spectrometer for $\Delta^{14}C$ analysis. HPLC-RI is a simple and well-established method for carbohydrate analysis; however, in environmental studies, it has been less explored [27,45] than traditional GC-MS or high-performance anion-exchange chromatography with pulsed amperometric detection (HPAEC-PAD) techniques [5,8,10,11,31,46,47].

This study employs HPLC-RI to demonstrate that four successive purifications on Na^+, Ca^{2+}, Pb^{2+}, and Ca^{2+} cation-exchange columns are sufficient to produce pure carbohydrates for compound-specific carbon isotope determination. In previous investigations, the isolated fractions were measured after combustion in evacuated quartz tubes and the produced CO_2 was purified on vacuum lines. This was followed by graphitization for solid measurements or transfer in glass ampoules for gas measurements. On the other hand, this study employs an alternative procedure [48] based on the direct combustion of isolated fractions using an elemental analyzer coupled to the gas source of a mini carbon dating system (AixMICADAS) for $\Delta^{14}C$ analysis. Compared to the time-consuming vacuum line method, this procedure is relatively fast and can be adapted for sample masses $\leq$10 μg C with moderate precision. The applicability of the method was tested on two different environmental samples, namely marine particulate organic matter (POM) and total suspended atmospheric particles (TSP).

2. Materials and Methods

2.1. Chemicals and reagents

All the carbohydrate standards used in this study were purchased from Sigma-Aldrich or Interchim at the purest available grade (>98%). The standard stock

solutions of the individual (1 mM) and a mixture of 14 monosaccharides (glucose, galactose, mannose, fucose, rhamnose, arabinose, xylose, fructose, xylitol, sorbitol, mannitol, levoglucosan, mannosan, and galactosan, 1 mM and 50 µM each) were prepared by dilution with ultrapure water. The prepared solutions were stored in the dark at –15 °C until use. HCl (37%, Sigma-Aldrich), diluted with ultrapure water (final concentration of 1 M), was used for sample hydrolysis. The ultrapure water used in this work was produced by a Millipore Milli-Q system (Molsheim, France).

2.2. Sampling and carbohydrate extraction

2.2.1. Marine POM

Sinking particles (marine POM) were collected over seven-day periods from January 6th to March 3th, 2013, in the upwelling system located offshore Lima (Peru) in the Pacific Ocean (12° 02’ S - 77° 40’ W), using sediment traps (PPS3, Technicap) deployed in the oxycline/upper oxygen minimum zone (OMZ) layer at a depth of 34 m [49]. To avoid POM bio-degradation, a solution of seawater with 5% formaldehyde was added to the bottom of the collection chamber. After trap recovery, the living and dead swimmers were carefully removed so that only detrital particles remained in the sample. These detrital particles (marine POM) were stored in the dark at 4 °C in the initial chambers used in the PPS3. On land, the samples were filtered through 25 mm pre-combusted (450 °C, 6 h) Whatman GF/F filters (nominal retention size, 0.7 µm), freeze-dried, and subsequently stored in the dark at 4 °C until further analysis. The organic carbon (OC) content of the particles was in the range 20–29%. To obtain sufficient material for isotopic analysis, five portions (40–60 mg each) of each of the five samples obtained from the respective collection chambers of the sediment trap were pooled together. This resulted in ~265 mg dry POM powder which was hydrolyzed with 1 M HCl at 100 °C for 20 h [50]. The acid-soluble fraction recovered after

centrifugation (2000 rpm) was then transferred into a pre-combusted (450 °C, 6 h) glass vial and the acid was removed from the sample by three successive lyophilizations. The afforded dry powder was weighed (25.61 mg), redissolved in 1 mL ultrapure water and filtered through a Pasteur pipette packed with quartz wool (both pre-combusted at 450 °C for 6 h) to remove any remaining particles prior to chromatographic injection.

2.2.2. TSP

The aerosol sample was collected on a pre-combusted (450 °C, 6 h) weighed Whatman quartz fiber filter (20.3 cm × 25.4 cm) using an automatic sampler (Tisch Environmental USA; flow rate 85 m^3 h^{-1}). The sample was collected from the 10th to 17th March, 2016, from the rooftop of the Endoume marine station (Marseille; 43° 16' N - 5° 21' E). After collection, the sample was dried for 24 h in a desiccator, weighed, and then stored in a freezer at –25 °C in pre-combusted aluminum foil (450 °C, 6 h). Three portions (17.34 cm^2 each) of the filter were extracted with 18 mL ultrapure water in an ultrasonic bath for 1 h and then filtered through a Pasteur pipette packed with quartz wool (both pre-combusted at 450 ˚C for 6 h) to remove any remaining particles [5]. Finally, the sample was freeze-dried and stored in a freezer at –35 °C until chromatographic injection.

2.3. Chromatography

The carbohydrates were analyzed using an HPLC system (Thermo Scientific UltiMate 3000) equipped with a vacuum degasser and a 100-µL loop auto-injector. The carbohydrates were detected with a refractive index detector (Shodex RI-101) and eluted in isocratic mode with ultrapure water, which was previously degassed with high purity N_2 for 30 min.

Three cation-exchange analytical columns packed with a polymeric resin (sulfonated polystyrene-divinyl benzene) were used to purify the carbohydrates (Table S.1). The

first column (Na^+: 4% cross-linked Na^+; 200 × 10 mm, 12 µm; REZEX™ RNO-Oligosaccharide; Phenomenex) was used to separate the oligosaccharides from the monosaccharides after acid hydrolysis. The column temperature was set at 85 °C and the carbohydrates were eluted with ultrapure water at a flow rate of 0.3 mL min^{-1}. The second column (Ca^{2+}: 8% cross-linked Ca^{2+}; 300 × 7.8 mm, 9 µm; REZEX™ RCM-Monosaccharide; Phenomenex) was used to separate the neutral sugars from sugar alcohols and anhydrosugars. The column temperature was maintained at 85 °C throughout the analysis at a flow rate of 0.6 mL min^{-1}. The third column (Pb^{2+}: 8% cross-linked resin Pb^{2+}; 300 × 7.8 mm, 8 µm; REZEX™ RPM-Monosaccharide; Phenomenex) was used to further separate the monosaccharides at 75 °C and a flow rate of 0.6 mL min^{-1}. The injected samples never exceeded 10 mg/injection and the columns were cleaned at the end of each day by washing overnight with ultrapure water at a flow rate of 0.1 mL min^{-1}. The carbohydrate fractions and/or individual monosaccharides were collected by an automatic Foxy R1 fraction collector (Teledyne ISCO, USA) placed after the RI detector. The system was controlled via Chromeleon chromatography software (Thermofisher).

The detection limit of the HPLC-RI system was ~1 µM at a signal-to-noise ratio (S/N) of three for all the carbohydrates on the three tested columns; this was in agreement with previous results reported in the literature [51]. The precision of the method was evaluated by calculating the relative standard deviation (RSD%) for six replicate HPLC-RI injections of the standard mixture of the 14 carbohydrates at the 5 µM level. The RSD was <10% for the peak area and <1% for the retention time for all the columns tested. Additional details on the system optimization are included in the supplementary information (section S1 and Fig. S1).

2.4. Isotopic measurements

215 2.4.1. EA-IRMS

216 Prior to EA-IRMS processing, the samples were acidified with HCl (final
217 concentration, 0.01 M) to avoid any errors related to the isotopic signature of inorganic
218 carbon mainly from atmospheric CO_2 absorbed in the sample [52]. The samples were
219 placed in a tin capsule (5 mm × 9 mm; light; Santis) and dried under a N_2 stream. The
220 stable carbon isotope composition and the carbon content of the purified carbohydrates
221 were measured using an elemental analyzer (Flash EA 1500; Thermo Finnigan,
222 Germany) coupled with an isotope ratio mass spectrometer (IRMS Delta^{plus}, Thermo
223 Finnigan, Germany). Briefly, this technique measures the $^{13}C/^{12}C$ ratio of total carbon of
224 the dried sample as follows: in a continuous helium flow, the sample is oxidized at 1000
225 °C in the presence of O_2 and catalysts; the resulting CO_2 is separated from the other
226 combustion products and transferred by the helium flow to a gas source, magnetic
227 sector, triple collector mass spectrometer. The latter determines the $^{13}C/^{12}C$ ratio of
228 CO_2-carbon. The stable carbon isotope composition is conventionally expressed as $\delta^{13}C$
229 values according to the formula:

$$\delta^{13}C\ ‰ = \left[\frac{(^{13}C/^{12}C)_{Sample}}{(^{13}C/^{12}C)_{\mathrm{VPDB}}} - 1\right] \times 1000$$

230 where VPDB is the Vienna Pee Dee Belemnite standard.

231 International Atomic Energy Agency (IAEA)-CH-7 polyethylene ($\delta^{13}C = -32.2‰$)
232 and IAEA-CH-6 sucrose were used as the calibration standard and control, respectively
233 [53]. The latter yielded a mean value of −10.5‰. The $\delta^{13}C$ and carbon content of the
234 samples were corrected for the contribution of carbon in the tin capsules. The $\delta^{13}C$
235 standard deviations were determined from replicated measurements of the IAEA-CH-6
236 standard and were ± 0.2‰, ± 0.2‰, ± 0.4‰, and ± 0.7‰ for samples containing 20, 10,

5, and 2 µg C, respectively. The precision on the carbon content (precision on the absolute amount of carbon analyzed) was ± 0.1 µg C.

2.4.2. EA-AixMICADAS

Direct radiocarbon measurement of the CO_2 gas was carried out, after combustion, using an elemental analyzer (EA) coupled to the gas interface system (GIS) of the AixMICADAS system [48]. Briefly, the main characteristic of the EA is that it works with a combustion tube filled with tungsten oxide heated to 1050 °C to allow the introduction of silver boats containing the sample material. The purified extracts were recovered in ultrapure water without acidification, transferred into silver capsules (4 mm × 8 mm, Elemental Microanalysis Ltd), and dried at 80 °C on a hotplate under a N_2 stream. The silver capsules were baked at 800 °C for 3 h prior to use to eliminate any organic contamination [54,55]. The CO_2 produced by the EA is captured in the zeolite trap inside the GIS. The CO_2 is then released by heating the zeolite trap to 450 °C and is mixed inside the syringe with a helium flow in order to obtain 5% CO_2 in the gas mixture, which is sputtered into the ion source. The CO_2 is injected from the GIS into the ion source through a small fused silica capillary continuously fed by the syringe, which is driven by a stepping motor controlled by the GIS software. A carbon flow of 2.80 µg C min^{-1} keeps the total pressure constant inside the syringe (filled to 1300 mbar), allowing the ion source to produce stable currents. The tuning procedure and main operation parameters used in the gas configurations are described in the literature [48]. The measurements were normalized with the oxalic acid 2 standard (~100 µg C; OxA2 SRM 4990 C, National Institute of Standards and Technology) and corrected for blanks using phthalic anhydride acid ($F^{14}C$ = 0.0027; n = 3) prepared from the same protocol as that used for OxA2 (i.e. silver capsules measured by EA-GIS).

The samples were blank corrected with procedural blanks of the same size (section 3.3) and a conservative uncertainty of 30% of the blank value was propagated in the final error calculation. The samples were in the size range 50–150 μg C, which translates to a precision of ~1% for a modern sample. However, samples down to 10 μg C could be measured with less precision. The accuracy of ^{14}C measurements of small samples (< 100 μg C) with the gas ion source of AixMICADAS has been tested with numerous measurements on various standards (NIST 4990C, IAEA-C1, IAEA-C2, in-house carbonate standards) [54,55]. For example, the analysis of oxalic acid NIST 4990C was replicated 132 times over 2.5 years, giving an average $F^{14}C$ of 1.3403 and a standard deviation (SD) of 0.0078 (i.e. 6‰). This arithmetic mean and its associated error (std error = 0.0007) are compatible with the weighted mean (1.3405) and the weighted error (0.0008), and closely agree with the NIST reference value of 1.3407 ± 0.0005.

The ^{14}C analyses were reported as $\Delta^{14}C$ corrected for decay [56,57] according to the formula:

$$\Delta^{14}C\ ‰\ (corrected\ for\ decay) = \left(\frac{A_{SN} e^{\lambda_c\,(1950\,-X)}}{A_{ON}} - 1\right) \times 1000$$

where A_{SN} is the normalized sample activity, A_{ON} is the normalized standard activity, x is the year of formation or growth, and $\lambda_C = (1/8267)\ yr^{-1}$.

2.5. Identification of purified monosaccharides

The identification of the isolated purified monosaccharides was checked with Liquid Chromatography coupled with Time-of-Flight Mass Spectrometry (LC-Q-TOF-MS) Agilent 6500 system. The chromatographic separation was performed with a Luna HILIC column (100 mm × 2.00 mm I.D., 3 μm particle size; Phenomenex). The mobile phase was ultrapure water with 13 mM CH_3COONH_4 (A) and acetonitrile (LC-MS

grade) with 13 mM CH_3COONH_4 (B) and sugars were eluted isocratically (20% A and 80% B). The flow rate and the column temperature were set at 200 μL min^{-1} and 25 ºC, respectively for the whole run. Monosaccharides were injected without prior derivatization and ionized in the ESI positive mode. The main ion source parameters were optimized as follows: source temperature 350 ºC, sheath gas temperature 350 ºC, gas flow 11 L min^{-1}, and drying gas at 8 L min^{-1}. The MS scan was 50 – 1700 m/z, and the scan rate was 1 spectra s^{-1}. The capillary voltage and the nozzle voltage were set at 4000 V and 500 V, respectively. Samples and standards were diluted in acetonitrile before injection.

3. Results and discussion

3.1. Cation-exchange column selection and purification procedure

Cation-exchange chromatography allows the separation of poly-, oligo-, and monosaccharides based on their degree of polymerization [45,58]. The chromatographic resolution and selectivity can be modulated by changing the cation-exchange column. The separation mechanism is based on the strength of the complex formed between the hydroxyl groups of the carbohydrate and the metal (e.g. K^+, Na^+, Pb^{2+}, Ca^{2+}, Cd^{2+}, and Cu^{2+}).

In this study, Na^+, Ca^{2+}, and Pb^{2+} columns were selected for optimum purification of the set of studied carbohydrates. The Na^+ column is ideal to separate polysaccharides from oligosaccharides and monosaccharides, whereas the Ca^{2+} and Pb^{2+} columns provide further and complementary separation among the different monosaccharides (e.g. neutral monosaccharides, alditols, anhydrosugars; Fig. 1 a-c). Compared to NH_2^- columns (also employed for sugar preparative chromatography), Na^+, Ca^{2+}, and Pb^{2+} columns have the advantage of running with ultrapure water as eluent instead of acetonitrile. This considerably reduces the organic carbon contamination delivered by

309 the eluent, while ultrapure water is easily removed by evaporation with a minimum
310 organic carbon background left behind.

311 Because carbohydrates in environmental samples can also be polymers
312 (polysaccharides and oligosaccharides) and acid hydrolysis is not always 100%
313 effective [59], an initial purification on a Na^+ column was necessary to separate the
314 polymers from the monosaccharides [60]. The next step was the sequential purification
315 of the monosaccharides on the Ca^{2+}, Pb^{2+} and again, when necessary, on the Ca^{2+}
316 columns. This provided further and complementary separation among the different
317 monosaccharides (e.g. neutral monosaccharides, alditols, anhydrosugars; Fig. 1 b-c)
318 [61]. In summary the purification procedure flowchart proposed in this study is: $Na^+ \rightarrow$
319 $Ca^{2+} \rightarrow Pb^{2+} \rightarrow Ca^{2+}$.

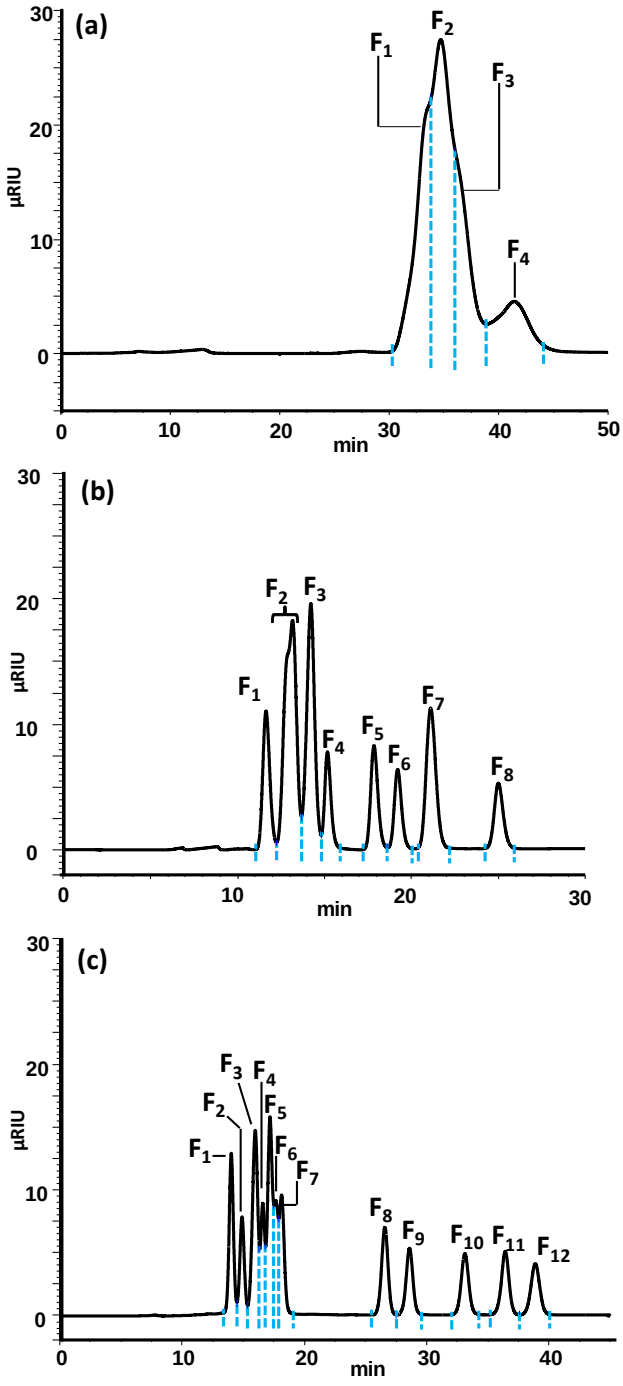

Fig. 1. Chromatogram of a standard monosaccharide mixture (1 mM each): (a) Na^+ column: F_1 (glucose + rhamnose + mannitol)/F_2 (xylitol + sorbitol + fructose + mannose + galactose + xylose)/F_3 (fucose + arabinose + galactosan)/F_4 (levoglucosan + mannosan); (b) Ca^{2+} column: F_1 (glucose)/F_2 (xylose + galactose + mannose + rhamnose)/F_3 (fucose + fructose + arabinose)/F_4 (galactosan)/F_5 (mannitol)/F_6 (levoglucosan)/F_7 (sorbitol + xylitol)/F_8 (mannosan); and (c) Pb^{2+} column: F_1 (glucose)/F_2 (xylose)/F_3 (galactose + rhamnose)/F_4 (galactosan)/F_5 (arabinose +

328 fucose)/F_6 (mannose)/F_7 (fructose)/F_8 (mannitol)/F_9 (levoglucosan)/F_{10} (xylitol)/F_{11}
329 (sorbitol)/F_{12} (mannosan). Dashed vertical lines correspond to the duration of the eluted
330 compound(s) and were used as the starting and ending points of peak collection by the
331 fraction collector.
332
333 *3.2. Monosaccharide standards purification and recovery yields*
334 The analytical procedure flowchart established in the previous section was tested on
335 monosaccharide standards (neutral monosaccharides, alditols, and anhydrosugars; initial
336 concentration of 50 µM) to evaluate the separation and peak isolation of the single
337 monosaccharides. The monosaccharide standards were sequentially purified on Ca^{2+} and
338 Pb^{2+} columns and if necessary, again on a Ca^{2+} column. Note that for the purpose of this
339 exercise the Na^{+} column was not included because the polysaccharides and
340 oligosaccharides were not considered in the standard (section 3.1).
341 The first separation was achieved on a Ca^{2+} column (Fig. S2 a) and resulted in eight
342 peaks corresponding to fractions F_1–F_8, which were collected into 6 mL pre-combusted
343 (450 °C, 6 h) glass tubes. The obtained results indicated that at this stage of the
344 purification process only the F_8 fraction (e.g. mannosan) was pure because it was eluted
345 significantly after the other monosaccharides (Fig. S2 a). Therefore, this
346 monosaccharide was not purified further. The collected fractions F_1–F_7 were freeze
347 dried, redissolved into 300 µL ultrapure water, and injected individually into the Pb^{2+}
348 column (Fig. S2 b). It is worth noting that fractions in the time periods between the two
349 adjacent peaks were also collected and their purity was checked after injection into the
350 Pb^{2+} column. The monosaccharide(s), if any, obtained in such a way was (were) further
351 pooled with fraction(s) that contained the same monosaccharide to increase its recovery.
352 Following the second purification, 10 peaks were obtained corresponding to fractions

353 F_1–F_{10}. The last purification was performed on a Ca^{2+} column to ensure the collection of
354 ultrapure monosaccharide targets (Fig. S2 c).

355 The obtained results revealed that the recovery yields after three successive
356 purifications (Ca^{2+}→ Pb^{2+} → Ca^{2+}) of the standard mixture ranged from 12.38 ± 0.01%
357 to 36.32 ± 0.02% (n = 3), with the highest values observed for glucose, mannosan,
358 levoglucosan, and mannitol and the lowest for arabinose (Table S2). Notably, for
359 environmental sample analysis (section 3.5), the monosaccharides xylose, fucose, and
360 rhamnose were also included in the standard (in total 14 monosaccharides) despite the
361 fact that their recovery yield was not estimated via this exercise.

362 *3.3. Chromatographic system blanks and background isotopic signature*

363 The blanks were run on the HPLC-RI system with ultrapure water and the amount of
364 carbon released from the chromatographic columns (column bleeding) and isotopic
365 signature were evaluated (Table 1). Column blanks were recorded during the whole run
366 for each column: 50 min for the Na^+ column, 30 min for the Ca^{2+} column, and 45 min
367 for the Pb^{2+} column. Subsequently, the amount of carbon released from these three
368 columns was measured via EA-IRMS. The obtained values were significantly close for
369 the Ca^{2+} and Pb^{2+} columns (4.84 ± 0.25 and 2.80 ± 0.21 µg, respectively), while those of
370 the Na^+ column were much higher (28.64 ± 1.57 µg). Despite these differences, all the
371 blanks resulted in a similar $\delta^{13}C$ signature ranging from −28.4 ± 0.4 to −27.8 ± 0.4‰
372 (Table 1).

373 The next step was to estimate the total carbon release after sequential purification on
374 the Na^+→ Ca^{2+}→ Pb^{2+}→ Ca^{2+} columns. The obtained results indicated that the
375 purification procedure produced a blank that contained 19.76 ± 1.80 µg carbon (Table
376 1) with a $\delta^{13}C$ value of −27.9 ± 1.1‰; these results were similar to those observed for
377 each column. Blanks corresponding to the collection time window of the three

monosaccharides (glucose, galactose, and levoglucosan) after $Na^+ \rightarrow Ca^{2+} \rightarrow Pb^{2+} \rightarrow Ca^{2+}$ purification were also run. The respective carbon inputs and the $\delta^{13}C$ signatures after $Na^+ \rightarrow Ca^{2+} \rightarrow Pb^{2+} \rightarrow Ca^{2+}$ purification were 0.58 ± 0.004 µg and −24.4 ± 2.9 ‰ for glucose and 0.54 ± 0.15 µg and −26.7 ± 1.5‰ for levoglucosan (Table 1).

Because of the elevated cost of radiocarbon analysis, radiocarbon blanks were only run for the collection time trap of the three monosaccharides (glucose, galactose and levoglucosan) measured in this study. Moreover, as the amount of carbon delivered for the whole purification procedure ($Na^+ \rightarrow Ca^{2+} \rightarrow Pb^{2+} \rightarrow Ca^{2+}$ columns) for each of the these monosaccharides was too small for a reliable $\Delta^{14}C$ measurement, phthalic acid (^{14}C free blank sample) was added to the final collected blank and the sample was processed as the monosaccharide sample (i.e. transferred into Ag capsules with ultrapure water and combusted by the EA coupled to the gas interface of AixMICADAS). The amount of phthalic acid was adjusted according to the size of the sample to correct for constant contamination offsets. The results revealed that the radiocarbon blanks exhibited values ranging from −988 to −986‰ (Table 1).

These $\Delta^{14}C$ values are slightly higher than those observed for the phthalic acid samples (≈ −997‰) measured directly after addition into the silver capsules (i.e. without any transfer from the collection tube to the silver cups). This suggests that little exogenous carbon was added to the sample from HPLC purification (column bleeding and organic residues), glassware contamination (collection vials, Pasteur pipets) and airborne particle deposition during sample collection and transfer. Moreover, the $\Delta^{14}C$ values (−989.7 ± 3.5‰) and carbon amounts (0.52 ± 0.34 µg C) of the ultrapure water samples (10 mL corresponding to ~10 times the volume of the collection window of a pure monosaccharide) indicated that the addition of exogenous carbon from the eluent was also negligible.

Table 1. Carbon content (µg), $\delta^{13}C$ (‰) and $\Delta^{14}C$(‰) values of the procedural blanks. Phthalic acid was added to the collected time window of the three monosaccharide samples and the ultrapure water sample to make the measurement feasible. The mass of phthalic acid was adjusted according to the sample mass of the respective time window of the examined environmental samples.

Blank	**Carbon** ± SD	$\delta^{13}C$ ± SD	$\Delta^{14}C$ ± SD
Na^+ column (n = 3) *	28.64 ± 1.57	−28.3 ± 0.8	ND
Ca^{2+} column (n = 3) *	4.84 ± 0.25	−28.4 ± 0.4	ND
Pb^{2+} column (n = 3) *	2.80 ± 0.21	−27.8 ± 0.4	ND
$Na^+ \rightarrow Ca^{2+} \rightarrow Pb^{2+} \rightarrow Ca^{2+}$ columns (n = 3)	19.76 ± 1.80	−27.9 ± 1.1	ND
Retention time window of glucose (n = 3) **	0.58 ± 0.00	−24.4 ± 2.9	−986.2 ± 5.8§
Retention time window of galactose (n = 2) **	< 2 ± 2.0†	ND	−988.2 ± 3.1
Retention time window of levoglucosan (n = 3) **	0.54 ± 0.15	−26.7 ± 1.5	−988.2 ± 0.9‡
Ultrapure water (n = 3)	0.52 ± 0.34	−21.9 ± 5.9	−989.7 ± 3.5

ND: Not determined
* Measured for the whole HPLC -RI run time for each column (Table S1)
** Measured for the whole purification procedure ($Na^+ \rightarrow Ca^{2+} \rightarrow Pb^{2+} \rightarrow Ca^{2+}$)
§ n = 4
† Measured with EA-AixMICADAS
‡ n = 2

Despite the significantly low amount of contaminants (< 1% for both the glucose and levoglucosan samples from the estimated carbon content of the retention time window) and the low $\Delta^{14}C$ procedural blanks, the results presented in this study were blank corrected. Finally, it is worth noting that the direct combustion of the small silver cups via an elemental analyzer allows a low background (equivalent age of 46 000 yr BP) and is therefore a good alternative to the time-consuming conventional method based on purification with a vacuum line.

Overall, the above results clearly suggest that the proposed purification procedure does not induce any significant contamination in the samples or affect their isotopic signature.

3.4. Hydrolysis effects

The marine sample was submitted to hydrolysis (1 M HCl) prior to its chromatographic purification (Section 2) to release the monosaccharides from the biopolymer macrostructure. Moreover, additional experiments were performed on the standard mono- and polysaccharides to investigate whether the hydrolysis conditions affect the isotopic composition of the released monosaccharides. The three levoglucosan standard solutions (90 µg C each) presented similar $\delta^{13}C_{levo}$ values, namely −11.2 ± 0.2‰ (n = 3) and −11.2 ± 0.1‰ (n = 3) before and after hydrolysis, respectively. Similar results were obtained by Wang et al. [19] for the glucose standard ($\delta^{13}C_{glc}$ = −9.8‰ and $\delta^{13}C_{glc}$ = −9.9‰ before and after processing, respectively); however their study included additional purification steps comprising anion and cation-exchange resins.

In another set of experiments a polysaccharide standard (laminarin) containing glucose units was submitted to acid hydrolysis and the isotopic signature of the released glucose was compared to that of the original laminarin. The results indicated that glucose and laminarin exhibited similar isotopic signatures in terms of $\delta^{13}C$ ($\delta^{13}C_{glc}$ = −10.4‰ and $\delta^{13}C_{lam.}$ = −13.0‰; n = 1) and $\Delta^{14}C$ ($\Delta^{14}C_{glc}$ = −85.4‰ and $\Delta^{14}C_{lam.}$= −84.90‰; n = 1) indicating few differences between the isotopic composition of the original polysaccharide and its monomeric constituent (Repeta; unpublished results).

3.5. Application to environmental samples

The purification procedure, including sample preparation, employed in this study is briefly summarized in Fig. 2. Two distinct environmental samples, namely, a marine POM and a TSP sample were considered. The choice of samples was made with respect

to the opportunities and the logistics set to obtain them but more importantly of their high carbohydrate content.

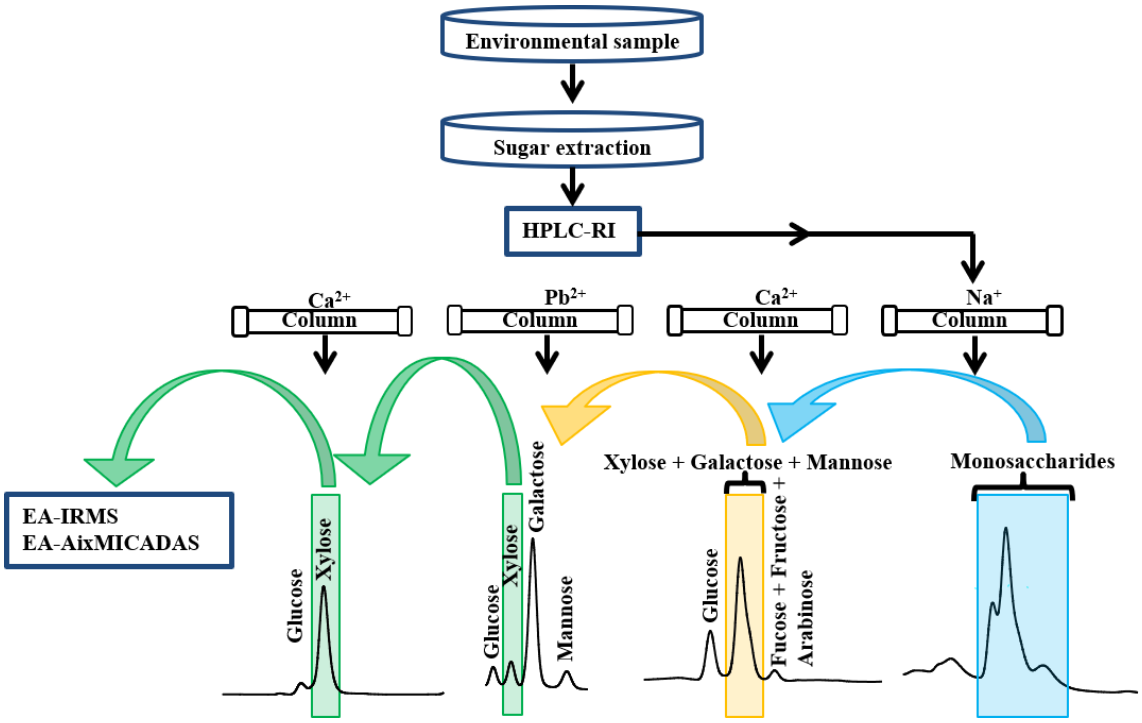

Fig. 2. Procedural flowchart of this study with a simplified example of the purification of xylose isolated from the marine particulate organic matter (POM) sample. The last purification of xylose on the Ca^{2+} was obtained after pooling the xylose fraction collected from the Pb^{2+} column and the xylose purified from the adjacent fractions.

3.5.1. Marine POM

The hydrolyzed marine sample was processed on a Na^{+} column and the collected fractions (F_3–F_6), corresponding to the monosaccharides, were further purified on Ca^{2+}→ Pb^{2+}→ Ca^{2+} columns (Fig. 3). The results indicated that after four sequential purifications the major monosaccharides obtained were: galactose (368 µg), glucose (273 µg), mannose (65 µg), xylose (38 µg), and fucose/arabinose (16 µg). It is worth noting that levoglucosan (1.8 µg) and mannosan (1.5 µg) were also collected for the

467 first time from marine POM; however, in very low amounts. The presence of the
468 abovementioned anhydrosugars in the hydrolyzed marine sample was also confirmed by
469 high-performance anion-exchange chromatography (Nouara et al., s*ubmitted*). Finally,
470 although rhamnose and galactosan were detected in the marine POM sample they
471 yielded very small recovered amounts (< 0.5 µg), which were insufficient for isotopic
472 measurement.

473 The results revealed that the marine POM sample exhibited a δ^{13}C value of −19.6 ±
474 0.6‰ which is typical of marine origin and consistent with the δ^{13}C values reported for
475 the surface coastal sinking POM (range: –23 to –20 ‰) [18,62]. The δ^{13}C signature of
476 the POM hydrophilic extract (fraction comprising most of the hydrophilic components
477 of the sample including monosaccharides) was slightly enriched (−17.2 ± 0.5‰)
478 compared to that of the bulk POM and agreed well with the δ^{13}C values recorded for
479 glucose, galactose, mannose, xylose, and fucose/rhamnose (−18.5 to −16.8‰; Table 2).

480 The δ^{13}C signature recorded for these individual monosaccharides agrees well with
481 the isotopic values measured for the individual monosaccharides in marine high-
482 molecular-weight dissolved organic matter (HMWDOM) [27], and thereby pointing
483 toward a marine origin. The slight depletion of the δ^{13}C values of the bulk POM relative
484 to its individual carbohydrate component may be due to the presence of other organic
485 compounds (e.g. amino acids and lipids) in the sample, which may have a lighter stable
486 carbon isotope signature than that observed for carbohydrates [20,22]. Regardless,
487 further molecular level isotopic analysis on individual amino acids and/or lipids is
488 warranted to test this hypothesis.

489 On the other hand, the levoglucosan (−27.2‰) and mannosan (−26.2‰) isotopic
490 signatures exhibited depleted δ^{13}C values when compared to those of the other
491 monosaccharides, indicating the different origin of these two monosaccharides (Table

2). Indeed, these sugars are well known tracers of terrestrial biomass burning processes [39], and thus their presence in marine POM indicates an external terrestrial input probably via atmospheric deposition [5,10] from C3 land plant tissue ($\delta^{13}C$: −32 to −20‰; mean: −27‰ [63]). The presence of levoglucosan and mannosan in the POM sample is not surprising since the sampling site was located a few kilometers offshore from the Lima area (section 2.2).

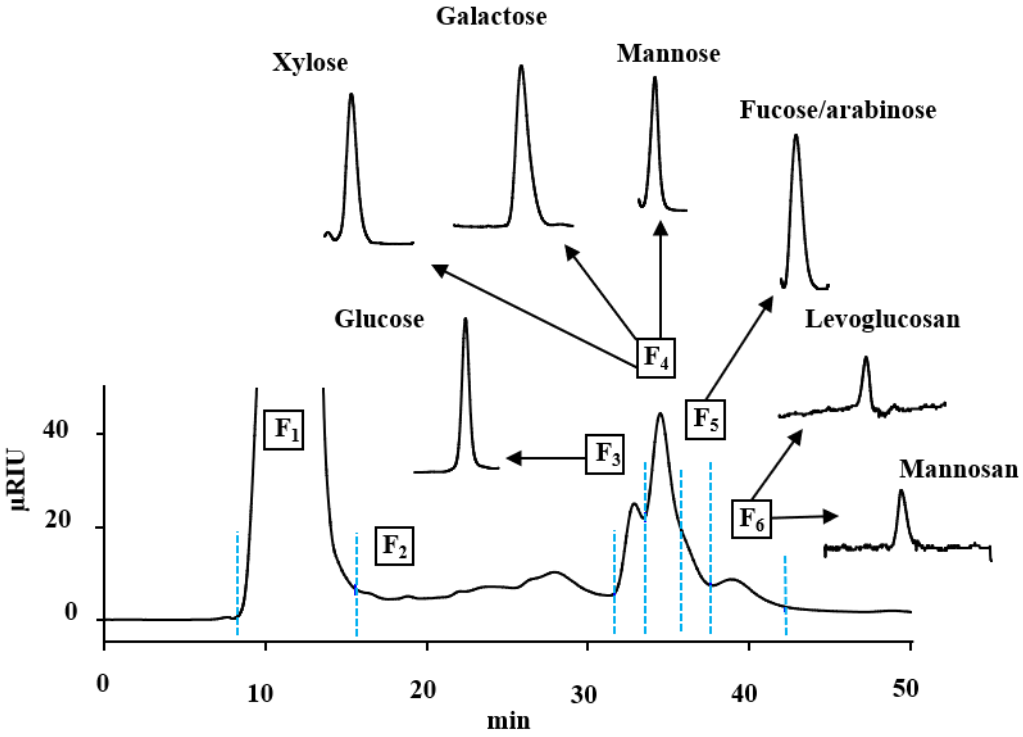

Fig. 3. Chromatogram of a marine particulate organic matter (POM) sample on a Na^+ column (F_1: polysaccharides; F_2: oligosaccharides; F_3: glucose, rhamnose; F_4: xylose, galactose, and mannose; F_5: fucose + arabinose, and galactosan; F_6: mannosan and levoglucosan). The final purified compounds (after $Na^+ \rightarrow Ca^{2+} \rightarrow Pb^{2+} \rightarrow Ca^{2+}$ purification) are also indicated with arrows.

The radiocarbon results of this study indicated that relatively to its hydrophilic fraction ($\Delta^{14}C$ = 124 ± 5‰), the marine POM sample was depleted ($\Delta^{14}C$ = 28 ± 8‰).

This agrees very well with previous investigations, which have reported similar results for a wide variety of environmental samples comprising sediments, sinking POM, planktons [19,64] including riverine, and marine HMWDOM [22,65]. Intermediate radiocarbon values were recorded for glucose and galactose ($\Delta^{14}C_{glc}$ = 43‰ and $\Delta^{14}C_{gal}$ = 19‰; Table 2) and are consistent with the radiocarbon monosaccharide signature reported for surface marine HMWDOM [27].

Table 2. $\delta^{13}C$ (‰) ± SD and $\Delta^{14}C$ (‰) ± SD values of the examined environmental samples. The $\Delta^{14}C$ values of galactose, glucose and levoglucosan are blank-corrected.

Sample	**Bulk OM** [§]	**Hydrophilic OM** [§] **extract**	**Pure monosaccharides**		
	$\delta^{13}C$ / $\Delta^{14}C$ (n = 3)	$\delta^{13}C$/ $\Delta^{14}C$ (n = 3)		$\delta^{13}C$ (n = 3)	$\Delta^{14}C$ ± 1 σ
POM	−19.6 ± 0.6 / 28 ± 8	−17.2 ± 0.5 / 124 ± 5	Mannose	−17.6 ± 0.9	−
			Xylose	−16.8 ± 0.2	−
			Fuc./Ara. [§§]	−18.5 ± 0.5	−
			Galactose	−16.9 ± 0.1	18.9 ± 16.3 (n = 3)**
			Glucose	−17.6 ± 0.1	43.3 ± 9.9 (n = 1)
			Levoglucosan	−27.2 [*]	−
			Mannosan	−26.2 [*]	−
TSP	−25.9 ± 0.0 / −175 ± 5	−24.8 ± 0.1 / −64 ± 13	Glucose	−25.1 ± 0.1	−
			Fructose	−25.3 ± 0.3	−
			Levoglucosan	−25.0 ± 0.4	33.0 ± 9.7 (n = 1)
			Mannosan	−25.7 ± 0.5	−
			Mannitol	−26.4 [*]	−

[§] Organic matter
[§§] Fucose / Arabinose
[*] n = 1
[**] $\Delta^{14}C$ ± SD

Overall, the above radiocarbon data indicate a modern age for the purified monosaccharides that further support the hypothesis that these monosaccharides are incorporated into a common family of polysaccharides (acylpolysaccharides) present in all terrestrial and aquatic ecosystems [66,67]. Nevertheless, more $\Delta^{14}C$ data on the

individual monosaccharides including other environmental matrices (e.g. sediments, and riverine POM and DOM) are warranted before any generalizations can be made.

3.5.2. TSP

The purification of the atmospheric sample was performed, without prior processing, on the Na^+ column. This was due to the low complexity of the sample and to avoid further possible losses and contamination that may occur during additional manipulation. The purification was conducted in a Ca^{2+} column, followed by a Pb^{2+} column and again by a Ca^{2+} column (Fig. 4). The obtained results indicated that after three purifications the major monosaccharides obtained were: levoglucosan (134 μg), fructose (40 μg), mannosan (38 μg), glucose (36 μg), and mannitol (4 μg). The abundance of these monosaccharides is in agreement with the results generally reported for PM_{10} particles [5,10]. Similar to the abovementioned results galactose, arabinose and galactosan were detected in the TSP sample. However, these were present in very low amounts (< 0.5 μg) and no isotopic measurements were performed.

The $\delta^{13}C$ value recorded for the TSP sample (−25.9 ± 0.0‰) was similar to that of its hydrophilic extract (−24.8 ± 0.1‰) and within the range of that of the isolated monosaccharides (−26.4 to −25.0‰; Table 2). These results reflect a dominant terrestrial origin from C3 vegetation and/or microorganisms, including fungal spores [6,37]. The $\delta^{13}C$ values of levoglucosan and mannosan were in agreement with the values reported by Sang et al. [25] for hardwood and stalk plant combustion. The $\delta^{13}C$ values reported in this study are also in good agreement with those measured for *n*-alkanes (C_{23}–C_{33}: −26.7 to −28.5‰), *n*-alkanols (C_{22}–C_{32}: −23.9 to −30.4‰), and long-chain *n*-alkanoic acids (C_{22}–C_{32}: −22.6 to −27.4‰) in the north western African dust over the Atlantic Ocean [41].

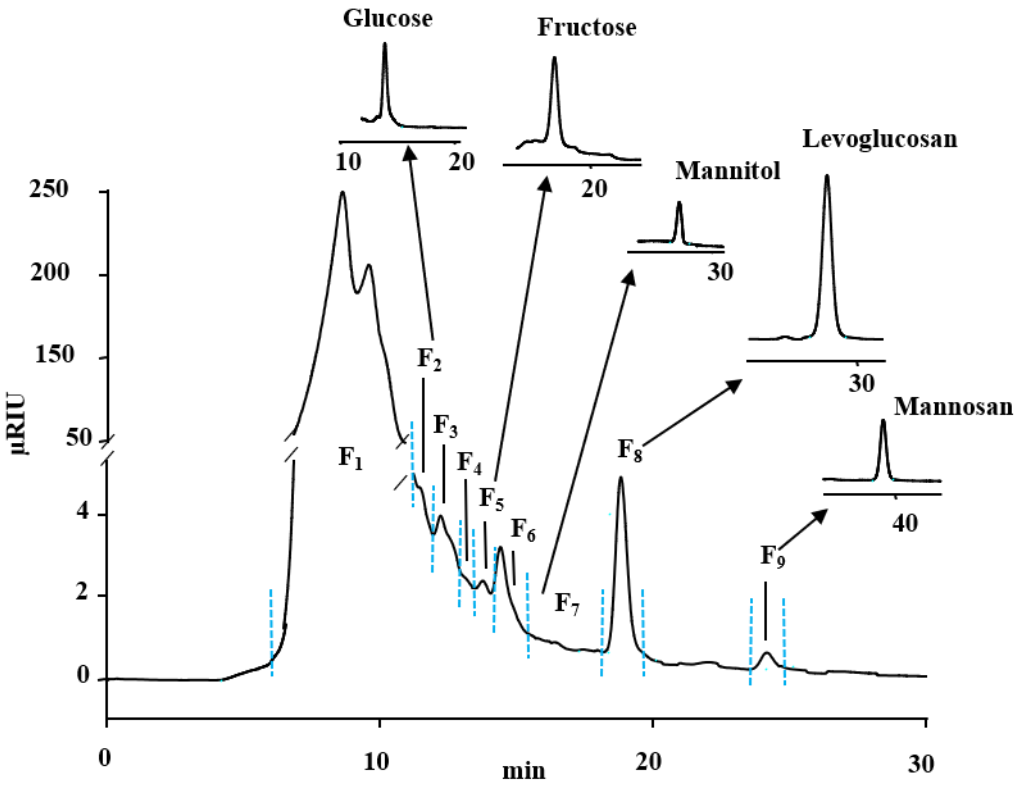

Fig. 4. Chromatogram of the total suspended atmospheric particles (TSP) on a Ca^{2+} column (F_1: polymer; F_2: glucose; F_3: unknown; F_4: galactose; F_5: arabinose and fructose; F_6: unknown and galactosan; F_7: mannitol; F_8: levoglucosan; F_9: mannosan). The final purified compounds (after $Ca^{2+}\rightarrow Pb^{2+}\rightarrow Ca^{2+}$ purification) are also indicated with arrows.

The radiocarbon signature of the TSP sample (Table 2) indicated that the bulk sample was highly depleted (−175 ± 5‰; 1545 yr) relative to its hydrophilic component (−64 ± 13‰; 530 yr). This is consistent with the characteristics already observed for the POM sample (section 3.5.1). The purified levoglucosan exhibited a modern radiocarbon age (33‰; Table 2), implying a very recent synthesis of this monosaccharide, which agrees with the radiocarbon signature of contemporary biosphere carbon ($\Delta^{14}C$ = 0 to 200‰) and concurs with the radiocarbon monosaccharide data of the marine POM sample. Although this result is a single and unique up-to-date measure of the $\Delta^{14}C$ of

levoglucosan, it can also explain, in part, the lack of stability of levoglucosan in the atmosphere over time since this compound has a modern age [68,69]. The radiocarbon signature of the TSP sample (1545 yr) relative to those of the purified water extract (530 yr) and levoglucosan (modern), may be due to the contribution of aged organic material such as black carbon (>50,000 yr). This material is known to be ubiquitous in the atmosphere as a result of fossil fuel emissions. This observation is further supported by the location of the sampling site (Marseille, France), which is characterized by the high influence from anthropogenic emissions and is in agreement with previous radiocarbon data performed on fossil fuels, soot aerosols, and $PM_{2.5}$ particles in other areas [70–72]. However, more TSP radiocarbon data in conjunction with compound specific radiocarbon analyses (i.e. monosaccharides, lipids, polyaromatic hydrocarbons) are required to confirm this hypothesis.

3.6. Identification of purified monosaccharides: comparison with authentic standards

Isolated monosaccharides recovered after the whole extraction and purification procedure were compared with authentic standards to check their purity. Depending on the amount of carbon recovered and the number of subsequently performed replicate EA-IRMS analysis, only three monosaccharides were further explored: levoglucosan, glucose, and galactose. The results from this study indicated that the mass spectra of the isolated monosaccharides well matched those of authentic standards (Table S3), as revealed by liquid chromatography coupled with quadrupole time-of-flight mass spectrometry (Q-TOF-LC/MS; Fig. S3). These results indicate that this proposed approach is specific, valid and reliable.

4. Conclusions and Outlook

590 The approach presented herein proved to be a powerful and robust tool for $\delta^{13}C$ and
591 $\Delta^{14}C$ determination of individual carbohydrates in the environmental matrices. Briefly,
592 after four successive purifications on cation-exchange columns, the pure carbohydrates
593 were produced and further assessed by EA-IRMS and/or EA-AixMICADAS. Particular
594 attention was given to the procedural blanks, which were found to be extremely low
595 during the whole cleanup procedure（0.5 μg C per carbohydrate collected).

596 The applicability of the proposed procedure was tested on two different
597 environmental samples comprising marine POM and TSP and the results revealed that
598 the isotopic compositions of the individual carbohydrates, in terms of $\delta^{13}C$, were in
599 good agreement with the data reported in the literature. Unfortunately, the $\Delta^{14}C$ values
600 for individual carbohydrates are scarce in literature and to the best of our knowledge,
601 only one study, on marine HMWDOM, has been reported to date. Therefore, we could
602 not directly compare the obtained results to $\Delta^{14}C$ values of similar samples.
603 Nevertheless, the obtained data suggested that the monosaccharides exhibit a modern
604 age, further implying the recent synthesis of these compounds and their rapid cycling.
605 Applying this method to a wide variety of environmental samples comprising marine
606 sediments, riverine organic matter, deep water HMWDOM, soils, and rain may
607 substantially help to improve the understanding of the carbohydrate dynamics and
608 organic matter cycling in all geochemical systems.

609 Finally, the overall approach highlights the high potential of preparative liquid
610 chromatography for application to the purification of specific compounds after selection
611 of the adequate column(s) for subsequent molecular-level isotopic measurements.
612 Moreover, future research employing two-dimensional cation-exchange
613 chromatography may prove to be a very useful tool to speed up the whole purification
614 procedure.

615

Acknowledgments

617 This research was funded by the projects AIOLOS, TRACFIRE (Labex OT-Med;
618 ANR-11-LABEX-0.061) and MANDARINE (grant No 2008-10372; Région Provence
619 Alpes Côte d'Azur). The project leading to this publication has received funding from
620 European FEDER Fund under project 1166-39417. The authors acknowledge the four
621 anonymous reviewers for valuable comments and fruitful discussions. A. Nouara was
622 supported by a Ph.D. grant from Aix-Marseille University.

623

Appendix A. Supplementary data

625 Supplementary data related to this article can be found at https://doi.org/10.1016/j.aca

Table and Figure captions

627 **Table 1.** Carbon content (µg), $\delta^{13}C$ (‰) and $\Delta^{14}C$(‰) values of the procedural blanks.
628 Phthalic acid was added to the collected time window of the three monosaccharide
629 samples and the ultrapure water sample to make the measurement feasible. The mass of
630 phthalic acid was adjusted according to the sample mass of the respective time window
631 of the examined environmental samples.

632

633 **Table 2.** $\delta^{13}C$ (‰) ± SD and $\Delta^{14}C$ (‰) ± SD values of the examined environmental
634 samples. The $\Delta^{14}C$ values of galactose, glucose and levoglucosan are blank-corrected.

635

Fig. 1. Chromatogram of a standard monosaccharide mixture (1 mM each): (a) Na^+ column: F_1 (glucose + rhamnose + mannitol)/F_2 (xylitol + sorbitol + fructose + mannose + galactose + xylose)/F_3 (fucose + arabinose + galactosan)/F_4 (levoglucosan + mannosan); (b) Ca^{2+} column: F_1 (glucose)/F_2 (xylose + galactose + mannose + rhamnose)/F_3 (fucose + fructose + arabinose)/F_4 (galactosan)/F_5 (mannitol)/F_6 (levoglucosan)/F_7 (sorbitol + xylitol)/F_8 (mannosan); and (c) Pb^{2+} column: F_1 (glucose)/F_2 (xylose)/F_3 (galactose + rhamnose)/F_4 (galactosan)/F_5 (arabinose + fucose)/F_6 (mannose)/F_7 (fructose)/F_8 (mannitol)/F_9 (levoglucosan)/F_{10} (xylitol)/F_{11} (sorbitol)/F_{12} (mannosan). Dashed vertical lines correspond to the duration of the eluted compound(s) and were used as the starting and ending points of peak collection by the fraction collector.

Fig. 2. Procedural flowchart of this study with a simplified example of the purification of xylose isolated from the marine particulate organic matter (POM) sample. The last purification of xylose on the Ca^{2+} was obtained after pooling the xylose fraction collected from the Pb^{2+} column and the xylose purified from the adjacent fractions.

Fig. 3. Chromatogram of a marine particulate organic matter (POM) sample on a Na^+ column (F_1: polysaccharides; F_2: oligosaccharides; F_3: glucose, rhamnose; F_4: xylose, galactose, and mannose; F_5: fucose + arabinose, and galactosan; F_6: mannosan and levoglucosan). The final purified compounds (after $Na^+ \rightarrow Ca^{2+} \rightarrow Pb^{2+} \rightarrow Ca^{2+}$ purification) are also indicated with arrows.

Fig. 4. Chromatogram of the total suspended atmospheric particles (TSP) on a Ca^{2+} column (F_1: polymer; F_2: glucose; F_3: unknown; F_4: galactose; F_5: arabinose and fructose; F_6: unknown and galactosan; F_7: mannitol; F_8: levoglucosan; F_9: mannosan).

661 The final purified compounds (after $Ca^{2+} \rightarrow Pb^{2+} \rightarrow Ca^{2+}$ purification) are also indicated
662 with arrows.
663

664 ## References

665 [1] J.I. Hedges, G.L. Cowie, J.E. Richey, P.D. Quay, R. Benner, M. Strom, B.R.
666 Forsberg, Origins and processing of organic matter in the Amazon River as
667 indicated by carbohydrates and amino acids, Limnol. Oceanogr. 39 (1994) 743–
668 761. doi:10.4319/lo.1994.39.4.0743.

669 [2] S. Opsahl, R. Benner, Characterization of carbohydrates during early diagenesis
670 of five vascular plant tissues, Org. Geochem. 30 (1999) 83–94.
671 doi:10.1016/S0146-6380(98)00195-8.

672 [3] C. Panagiotopoulos, D.J. Repeta, L. Mathieu, J.F. Rontani, R. Sempéré,
673 Molecular level characterization of methyl sugars in marine high molecular
674 weight dissolved organic matter, Mar. Chem. 154 (2013) 34–45.
675 doi:10.1016/j.marchem.2013.04.003.

676 [4] D.J. Repeta, Chemical characterization and cycling of dissolved organic matter,
677 in: D. A. Hansell and C. A. Carlson (Ed.), Biogeochem. Mar. Dissolved Org.
678 Matter, Elsevier Science, USA, 2015: pp. 21–63.

679 [5] C. Theodosi, C. Panagiotopoulos, A. Nouara, P. Zarmpas, P. Nicolaou, K.
680 Violaki, M. Kanakidou, R. Sempéré, N. Mihalopoulos, Sugars in atmospheric
681 aerosols over the Eastern Mediterranean, Prog. Oceanogr. 163 (2018) 70–81.
682 doi:10.1016/j.pocean.2017.09.001.

683 [6] P. Fu, K. Kawamura, M. Kobayashi, B.R.T. Simoneit, Seasonal variations of

684 sugars in atmospheric particulate matter from Gosan, Jeju Island: Significant
685 contributions of airborne pollen and Asian dust in spring, Atmos. Environ. 55
686 (2012) 234–239. doi:10.1016/j.atmosenv.2012.02.061.

687 [7] J.M. Oades, Soil organic matter and structural stability: mechanisms and
688 implications for management, Plant Soil. 76 (1984) 319–337.

689 [8] C. Panagiotopoulos, R. Sempéré, J. Para, P. Raimbault, C. Rabouille, B.
690 Charrière, The composition and flux of particulate and dissolved carbohydrates
691 from the Rhone River into the Mediterranean Sea, Biogeosciences. 9 (2012)
692 1827–1844. doi:10.5194/bg-9-1827-2012.

693 [9] J.D. Pakulski, R. Benner, Abundance and distribution of carbohydrates in the
694 ocean, Limnol. Oceanogr. 39 (1994) 930–940. doi:10.4319/lo.1994.39.4.0930.

695 [10] P. Fu, K. Kawamura, K. Miura, Molecular characterization of marine organic
696 aerosols collected during a round-the-world cruise, J. Geophys. Res. 116 (2011)
697 1–14. doi:10.1029/2011JD015604.

698 [11] R. Sempéré, M. Tedetti, C. Panagiotopulos, B. Charriere, F. Van Wambeke,
699 Distribution and bacterial availability of dissolved neutral sugars in the South
700 East Pacific, Biogeosciences. 5 (2008) 1165–1173. doi:10.5194/bg-5-1165-2008.

701 [12] S.R. Beaupré, The Carbon Isotopic Composition of Marine DOC, in: D.A.
702 Hansell, C.A. Carlson (Eds.), Biogeochem. Mar. Dissolved Org. Matter, Second
703 Edi, Academic Press, Boston, 2015: pp. 335–368.
704 doi:https://doi.org/10.1016/B978-0-12-405940-5.00006-6.

705 [13] E.A. Hobbie, R.A. Werner, Intramolecular, compound-specific, and bulk carbon
706 isotope patterns in C 3 and C 4 plants: a review and synthesis, New Phytol. 161

(2004) 371–385. doi:10.1046/j.1469-8137.2004.00970.x.

[14] J. Hwang, E.R.M. Druffel, Carbon isotope ratios of organic compound fractions in oceanic suspended particles, Geophys. Res. Lett. 33 (2006) 1–5. doi:10.1029/2006GL027928.

[15] D. López-Veneroni, The stable carbon isotope composition of PM2.5 and PM10 in Mexico City Metropolitan Area air, Atmos. Environ. 43 (2009) 4491–4502. doi:10.1016/j.atmosenv.2009.06.036.

[16] C.P. Bataille, M. Mastalerz, B.J. Tipple, G.J. Bowen, Influence of provenance and preservation on the carbon isotope variations of dispersed organic matter in ancient floodplain sediments, Geochemistry, Geophys. Geosystems. 14 (2013) 4874–4891. doi:10.1002/ggge.20294.

[17] P.K. Zigah, E.C. Minor, H.A.N. Abdulla, J.P. Werne, P.G. Hatcher, An investigation of size-fractionated organic matter from Lake Superior and a tributary stream using radiocarbon, stable isotopes and NMR, Geochim. Cosmochim. Acta. 127 (2014) 264–284. doi:10.1016/j.gca.2013.11.037.

[18] L.A. Roland, M.D. McCarthy, T. Guilderson, Sources of molecularly uncharacterized organic carbon in sinking particles from three ocean basins: A coupled Δ14C and δ13C approach, Mar. Chem. 111 (2008) 199–213. doi:10.1016/j.marchem.2008.05.010.

[19] X.-C. Wang, E.R.M. Druffel, S. Griffin, C. Lee, M. Kashgarian, Radiocarbon studies of organic compounds classes in plankton and sediment of the northeastern Pacific Ocean, Geochim. Cosmochim. Acta. 62 (1998) 1365–1378. doi:10.1016/S0016-7037(98)00074-X.

730 [20] J. Hwang, E.R.M. Druffel, Lipid-Like Material as the Source of the
731 Uncharacterized Organic Carbon in the Ocean?, Science. 299 (2003) 881–884.
732 doi:10.1126/science.1078508.

733 [21] X.-C. Wang, R.F. Chen, G.B. Gardner, Sources and transport of dissolved and
734 particulate organic carbon in the Mississippi River estuary and adjacent coastal
735 waters of the northern Gulf of Mexico, Mar. Chem. 89 (2004) 241–256.
736 doi:10.1016/j.marchem.2004.02.014.

737 [22] A.N. Loh, J.E. Bauer, E.R.M. Druffel, Variable ageing and storage of dissolved
738 organic components in the open ocean., Nature. 430 (2004) 877–881.
739 doi:10.1038/nature02780.

740 [23] B.E. Van Dongen, S. Schouten, J.S. Sinninghe Damsté, Carbon isotope
741 variability in monosaccharides and lipids of aquatic algae and terrestrial plants,
742 Mar. Ecol. Prog. Ser. 232 (2002) 83–92. doi:10.3354/meps232083.

743 [24] B. Glaser, Compound-specificstable-isotope (δ13C) analysis in soil science, J.
744 Plant Nutr. Soil Sci. 168 (2005) 633–648. doi:10.1002/jpln.200521794.

745 [25] X.F. Sang, I. Gensch, W. Laumer, B. Kammer, C.Y. Chan, G. Engling, A.
746 Wahner, H. Wissel, A. Kiendler-Scharr, Stable carbon isotope ratio analysis of
747 anhydrosugars in biomass burning aerosol particles from source samples,
748 Environ. Sci. Technol. 46 (2012) 3312–3318. doi:10.1021/es204094v.

749 [26] R. Zhu, Y.-S. Lin, J.. Lipp, T.B. Meador, K.-U. Hinrichs, Optimizing sample
750 pretreatment for compound-specific stable carbon isotopic analysis of amino
751 sugars in marine sediment, Biogeosciences. 11 (2014) 4869–4880.
752 doi:10.5194/bgd-11-593-2014.

753 [27] D.J. Repeta, L.I. Aluwihare, Radiocarbon analysis of neutral sugars in high-
754 molecular-weight dissolved organic carbon: Implications for organic carbon
755 cycling, Limnol. Oceanogr. 51 (2006) 1045–1053.
756 doi:10.4319/lo.2006.51.2.1045.

757 [28] D. Derrien, J. Balesdent, C. Marol, C. Santaella, Measurement of the 13C/12C
758 ratio of soil-plant individual sugars by gas chromatography/combustion/isotope-
759 ratio mass spectrometry of silylated derivatives, Rapid Commun. Mass Spectrom.
760 17 (2003) 2626–2631. doi:10.1002/rcm.1269.

761 [29] M.A. Teece, M.L. Fogel, Stable carbon isotope biogeochemistry of
762 monosaccharides in aquatic organisms and terrestrial plants, Org. Geochem. 38
763 (2007) 458–473. doi:10.1016/j.orggeochem.2006.06.008.

764 [30] T.C.W. Moerdijk-Poortvliet, H. Schierbeek, M. Houtekamer, T. van Engeland,
765 D. Derrien, L.J. Stal, H.T.S. Boschker, Comparison of gas
766 chromatography/isotope ratio mass spectrometry and liquid
767 chromatography/isotope ratio mass spectrometry for carbon stable-isotope
768 analysis of carbohydrates, Rapid Commun. Mass Spectrom. 29 (2015) 1205–
769 1214. doi:10.1002/rcm.7217.

770 [31] C. Panagiotopoulos, R. Sempéré, Analytical methods for the determination of
771 sugars in marine samples : A historical perspective and future directions, Limnol.
772 Oceanogr. Methods. 3 (2005) 419–454. doi:10.4319/lom.2005.3.419.

773 [32] T.C.W. Moerdijk-Poortvliet, L.J. Stal, H.T.S. Boschker, LC/IRMS analysis: A
774 powerful technique to trace carbon flow in microphytobenthic communities in
775 intertidal sediments, J. Sea Res. 92 (2014) 19–25.
776 doi:10.1016/j.seares.2013.10.002.

[33] H.T.S. Boschker, T.C.W. Moerdijk-Poortvliet, P. van Breugel, M. Houtekamer, J.J. Middelburg, A versatile method for stable carbon isotope analysis of carbohydrates by high-performance liquid chromatography/isotope ratio mass spectrometry., Rapid Commun. Mass Spectrom. 22 (2008) 3902–3908. doi:10.1002/rcm.3804.

[34] A. Basler, J. Dyckmans, Compound-specific δ13C analysis of monosaccharides from soil extracts by high-performance liquid chromatography/isotope ratio mass spectrometry, Rapid Commun. Mass Spectrom. 27 (2013) 2546–2550. doi:10.1002/rcm.6717.

[35] K.T. Rinne, M. Saurer, K. Streit, R.T.W. Siegwolf, Evaluation of a liquid chromatography method for compound-specific δ13C analysis of plant carbohydrates in alkaline media, Rapid Commun. Mass Spectrom. 26 (2012) 2173–2185. doi:10.1002/rcm.6334.

[36] R.S. Sevcik, R.A. Mowery, C. Becker, C.K. Chambliss, Rapid analysis of carbohydrates in aqueous extracts and hydrolysates of biomass using a carbonate-modified anion-exchange column, J. Chromatogr. A. 1218 (2011) 1236–1243. doi:https://doi.org/10.1016/j.chroma.2011.01.002.

[37] H. Bauer, M. Claeys, R. Vermeylen, E. Schueller, G. Weinke, A. Berger, H. Puxbaum, Arabitol and mannitol as tracers for the quantification of airborne fungal spores, Atmos. Environ. 42 (2008) 588–593. doi:10.1016/j.atmosenv.2007.10.013.

[38] P.M. Medeiros, M.H. Conte, J.C. Weber, B.R.T. Simoneit, Sugars as source indicators of biogenic organic carbon in aerosols collected above the Howland Experimental Forest, Maine, Atmos. Environ. 40 (2006) 1694–1705.

801 doi:10.1016/j.atmosenv.2005.11.001.

802 [39] B.R.T. Simoneit, Biomass burning — a review of organic tracers for smoke from
803 incomplete combustion, Appl. Geochemistry. 17 (2002) 129–162.
804 doi:10.1016/S0883-2927(01)00061-0.

805 [40] T.I. Eglinton, L.I. Aluwihare, J.E. Bauer, Ellen R.M.Druffel, A.P. Mcnichol, Gas
806 Chromatographic Isolation of Individual Compounds from Complex Matrices for
807 Radiocarbon Dating, Anal. Chem. 68 (1996) 904–912. doi:10.1021/ac9508513.

808 [41] T.I. Eglinton, G. Eglinton, L. Dupont, E.R. Sholkovitz, D. Montluc, C.M. Reddy,
809 Composition, age, and provenance of organic matter in NW African dust over the
810 Atlantic Ocean, Geochemistry Geophys. Geosystems. 3 (2002) 1525–2027.
811 doi:10.1029/2001GC000269.

812 [42] A. Ingalls, A. Pearson, Ten Years of Compound-Specific Radiocarbon Analysis,
813 Oceanography. 18 (2005) 18–31. doi:10.5670/oceanog.2005.22.

814 [43] M. Makou, T. Eglinton, C. McIntyre, D. Montluçon, I. Antheaume, V. Grossi,
815 Plant Wax n-Alkane and n-Alkanoic Acid Signatures Overprinted by Microbial
816 Contributions and Old Carbon in Meromictic Lake Sediments, Geophys. Res.
817 Lett. 45 (2018) 1049–1057. doi:10.1002/2017GL076211.

818 [44] A.L. Bour, B.D. Walker, T.A.B. Broek, M.D. McCarthy, Radiocarbon Analysis
819 of Individual Amino Acids: Carbon Blank Quantification for a Small-Sample
820 High-Pressure Liquid Chromatography Purification Method, Anal. Chem. 88
821 (2016) 3521–3528. doi:10.1021/acs.analchem.5b03619.

822 [45] C. Panagiotopoulos, D.J. Repeta, C.G. Johnson, Characterization of methyl
823 sugars, 3-deoxysugars and methyl deoxysugars in marine high molecular weight

824 dissolved organic matter, Org. Geochem. 38 (2007) 884–896.
825 doi:10.1016/j.orggeochem.2007.02.005.

826 [46] P.M. Medeiros, B.R.T. Simoneit, Analysis of sugars in environmental samples by
827 gas chromatography-mass spectrometry, J. Chromatogr. A. 1141 (2007) 271–
828 278. doi:10.1016/j.chroma.2006.12.017.

829 [47] X. Cheng, L.A. Kaplan, Simultaneous analyses of neutral carbohydrates and
830 amino sugars in freshwaters with HPLC-PAD, J. Chromatogr. Sci. 41 (2003)
831 434–438. doi: 10.1093/chromsci/41.8.434.

832 [48] E. Bard, T. Tuna, Y. Fagault, L. Bonvalot, L. Wacker, S. Fahrni, H.A. Synal,
833 AixMICADAS, the accelerator mass spectrometer dedicated to14C recently
834 installed in Aix-en-Provence, France, Nucl. Instruments Methods Phys. Res.
835 Sect. B Beam Interact. with Mater. Atoms. 361 (2015) 80–86.
836 doi:10.1016/j.nimb.2015.01.075.

837 [49] M. Bretagnon, A. Paulmier, V. Garcon, B. Dewitte, S. Illig, L. Coppola, F.
838 Campos, F. Velazco, C. Panagiotopoulos, A. Oschlies, J.M. Hernandez-ayon, H.
839 Maske, O. Vergara, I. Montes, P. Martinez, E. Carrasco, J. Grelet, Desprez-De-
840 Gesincourt, C. Maes, L. Scouarnec, Modulation of the vertical particles transfer
841 efficiency in the Oxygen Minimum Zone off Peru, Biogeosciences. 15 (2018) 1–
842 19. doi:10.5194/bg-15-1-2018.

843 [50] C. Panagiotopoulos, R. Sempéré, V. Jacq, B. Charrière, Composition and
844 distribution of dissolved carbohydrates in the Beaufort Sea Mackenzie margin
845 (Arctic Ocean), Mar. Chem. 166 (2014) 92–102.
846 doi:10.1016/j.marchem.2014.09.004.

847 [51] C. Cheng, C.-S. Chen, P.-H. Hsieh, On-line desalting and carbohydrate analysis
848 for immobilized enzyme hydrolysis of waste cellulosic biomass by column-
849 switching high-performance liquid chromatography, J. Chromatogr. A. 1217
850 (2010) 2104–2110. doi:10.1016/j.chroma.2010.01.084.

851 [52] E.S. Gordon, M.A. Goni, Sources and distribution of terrigenous organic matter
852 delivered by the Atchafalaya River to sediments in the northern Gulf of Mexico,
853 Geochim. Cosmochim. Acta. 67 (2003) 2359–2375. doi:10.1016/S0016-
854 7037(02)01412-6.

855 [53] T.B. Coplen, W.A. Brand, M. Gehre, M. Gröning, H.A.J. Meijer, B. Toman,
856 R.M. Verkouteren, After two decades a second anchor for the VPDB δ13C scale,
857 Rapid Commun. Mass Spectrom. 20 (2006) 3165–3166. doi:10.1002/rcm.

858 [54] T. Tuna, Y. Fagault, L. Bonvalot, M. Capano, E. Bard, Development of small
859 CO2 gas measurements with AixMICADAS, Nucl. Instruments Methods Phys.
860 Res. Sect. B Beam Interact. with Mater. Atoms. 437 (2018) 93–97.
861 doi:10.1016/J.NIMB.2018.09.012.

862 [55] Y. Fagault, T. Tuna, F. Rostek, E. Bard, Radiocarbon dating small carbonate
863 samples with the gas ion source of AixMICADAS, Nucl. Instruments Methods
864 Phys. Res. Sect. B Beam Interact. with Mater. Atoms. (2019).
865 doi:10.1016/J.NIMB.2018.11.018.

866 [56] M. Stuiver, H.A. Polach, Reporting of C-14 data - Discussion, Radiocarbon. 19
867 (1977) 355–363.

868 [57] P.J. Reimer, T.A. Brown, R.W. Reimer, Discussion: Reporting and calibration of
869 post-bomb C-14 data, Radiocarbon. 46 (2004) 1299–1304.

870 [58] S.J. Angyal, G.S. Bethell, R.J. Beveridge, The separation of sugars and of polyols
871 on cation-exchange resins in the calcium form, Carbohydr. Res. 73 (1979) 9–18.

872 [59] C. Panagiotopoulos, O. Wurl, Spectrophotometric and chromatographic analysis
873 of carbohydrates in marine samples, in: O. Wurl (Ed.), Pract. Guidel. Anal.
874 Seawater, 1st Editio, CRC Press, Boca Raton, 2009: p. 408.

875 [60] C. Nobre, M.J. Santos, A. Dominguez, D. Torres, O. Rocha, A.M. Peres, I.
876 Rocha, E.C. Ferreira, J.A. Teixeira, L.R. Rodrigues, Comparison of adsorption
877 equilibrium of fructose, glucose and sucrose on potassium gel-type and
878 macroporous sodium ion-exchange resins, Anal. Chim. Acta. 654 (2009) 71–76.
879 doi:10.1016/j.aca.2009.06.043.

880 [61] J.A. Vente, H. Bosch, A.B. De Haan, P.J.T. Bussmann, Comparison of sorption
881 isotherms of mono- and disaccharides relevant to oligosaccharide separations for
882 Na, K, and Ca loaded cation exchange resins, Chem. Eng. Commun. 192 (2005)
883 23–33. doi:10.1080/00986440590473254.

884 [62] E.R.M. Druffel, P.M. Williams, J.E. Bauer, J.R. Ertel, Cycling of dissolved and
885 particulate organic matter in the open ocean, J. Geophys. Res. Ocean. 97 (1992)
886 15639–15659. doi:10.1029/92JC01511.

887 [63] M.H. O'Leary, Carbon Isotopes in Photosynthesis:Fractionation techniques may
888 reveal new aspects of carbon dynamics in plants, Bioscience. 38 (1988) 328–336.

889 [64] X.C. Wang, E.R.M. Druffel, Radiocarbon and stable carbon isotope compositions
890 of organic compound classes in sediments from the NE Pacific and Southern
891 Oceans, Mar. Chem. 73 (2001) 65–81. doi:10.1016/S0304-4203(00)00090-6.

892 [65] X.-C. Wang, J. Callahan, R.F. Chen, Variability in radiocarbon ages of

biochemical compound classes of high molecular weight dissolved organic matter in estuaries, Estuar. Coast. Shelf Sci. 68 (2006) 188–194. doi:10.1016/J.ECSS.2006.01.018.

[66] L.I. Aluwihare, D.J. Repeta, R.F. Chen, A major biopolymeric component to dissolved organic carbon in surface sea water, Nature. 387 (1997) 166–169. doi:10.1038/387166a0.

[67] D.J. Repeta, T.M. Quan, L.I. Aluwihare, A. Accardi, Chemical characterization of high molecular weight dissolved organic matter in fresh and marine waters, Geochim. Cosmochim. Acta. 66 (2002) 955–962. doi:10.1016/S0016-7037(01)00830-4.

[68] C.F. Fortenberry, M.J. Walker, Y. Zhang, D. Mitroo, W.H. Brune, B.J. Williams, Bulk and Molecular-Level Characterization of Laboratory-Aged Biomass Burning Organic Aerosol from Oak Leaf and Heartwood Fuels, Atmos. Chem. Phys. Discuss. 60 (2017) 1–40. doi:10.5194/acp-2017-576.

[69] A. Bertrand, G. Stefenelli, C.N. Jen, S.M. Pieber, E.A. Bruns, B. Temime-Roussel, J.G. Slowik, A.H. Goldstein, I. El Haddad, U. Baltensperger, A.S.H. Prévôt, H. Wortham, N. Marchand, Evolution of the chemical fingerprint of biomass burning organic aerosol during aging, Atmos. Chem. Phys. Discuss. (2018) 1–33. doi:10.5194/acp-2017-1196.

[70] L. Bonvalot, T. Tuna, Y. Fagault, J.-L. Jaffrezo, V. Jacob, F. Chevrier, E. Bard, Estimating contributions from biomass burning and fossil fuel combustion by means of radiocarbon analysis of carbonaceous aerosols: application to the Valley of Chamonix, Atmos. Chem. Phys. Discuss. (2016) 1–39. doi:10.5194/acp-2016-351.

[71] Z. Niu, S. Wang, J. Chen, F. Zhang, X. Chen, C. He, L. Lin, L. Yin, L. Xu, Source contributions to carbonaceous species in PM2,5 and their uncertainty analysis at typical urban, peri-urban and background sites in southeast China., Environ. Pollut. 181 (2013) 107–114. doi:10.1016/j.envpol.2013.06.006.

[72] A. Andersson, R.J. Sheesley, M. Kruså, C. Johansson, Ö. Gustafsson, 14C-Based source assessment of soot aerosols in Stockholm and the Swedish EMEP-Aspvreten regional background site, Atmos. Environ. 45 (2011) 215–222. doi:10.1016/j.atmosenv.2010.09.015.

Appendix A

Supporting data and information for

Liquid Chromatographic isolation of individual carbohydrates from environmental matrices for stable carbon analysis and radiocarbon dating

Amel Nouara[1], **Christos Panagiotopoulos**[1]***, **Jérôme Balesdent**[2], **Kalliopi Violaki**[1], **Edouard Bard**[2], **Yoann Fagault**[2], **Daniel James Repeta**[3], **Richard Sempéré**[1]

[1]Aix Marseille Univ., Université de Toulon, CNRS, IRD, MIO UM 110, 13288, Marseille, France

[2]Aix Marseille Univ., CNRS, Collège de France, IRD, INRA, CEREGE UM34, 13545 Aix-en-Provence, France

[3]Department of Marine Chemistry and Geochemistry, Woods Hole Oceanographic Institution, Woods Hole, MA 02543, USA

*Corresponding author. Phone: +33 4 86 09 05 26;

E-mail : christos.panagiotopoulos@mio.osupytheas.fr

February 27th, 2019

Table of Contents

S 1. Optimization of the HPLC-RI system

During the optimization step, a systematic large negative peak was always observed in the chromatograms at 18-20 min (Fig. S1). Previous studies indicated that this peak is probably due to the presence of dissolved oxygen in the sample and can mask the eluted compounds at this time window or cause an increase in the baseline noise [1]. The peak intensity somehow decreased after sample degassing (with pure He) but was still significant at low sample concentrations. We overcame this problem by installing a degassing device (RFIC eluent degasser, Thermo Fisher) before the chromatographic column. We found that this device increases neither the back-pressure of the system nor the retention time of the carbohydrates. To shorten the analysis time of the carbohydrates, no guard columns were used in this study. However, as a precaution, an online polyether ether ketone (PEEK) filter equipped with a stainless-steel frit (pore size 0.5 µm) was placed just before the online degasser. The filter frit was cleaned regularly by sonication in a methanol bath, followed by sonication in ultrapure water, once per month and between each sample purification.

Moreover, to maximize the collection efficiency of carbohydrates, the tubing between the RI detector and the fraction collector was minimized. The delay time between the detector and the fraction collector was calculated using 1 mM of vitamin B_{12} without an analytical column. Further adjustments of the working flow rates (0.3 mL min^{-1} and 0.6 mL min^{-1} for Na^+ and Ca^{2+}/Pb^{2+} columns, respectively) were made with a glucose standard (50 µM). We found that the highest recovery (~80%) of the glucose was obtained with a delay time of 110 s for the Na^+ column, and 60 s for the Ca^{2+} and Pb^{2+} columns. These delay times were applied for all peak and fraction collections during the purification procedure either of standards or samples.

S. 2. Supplementary figures and table legends

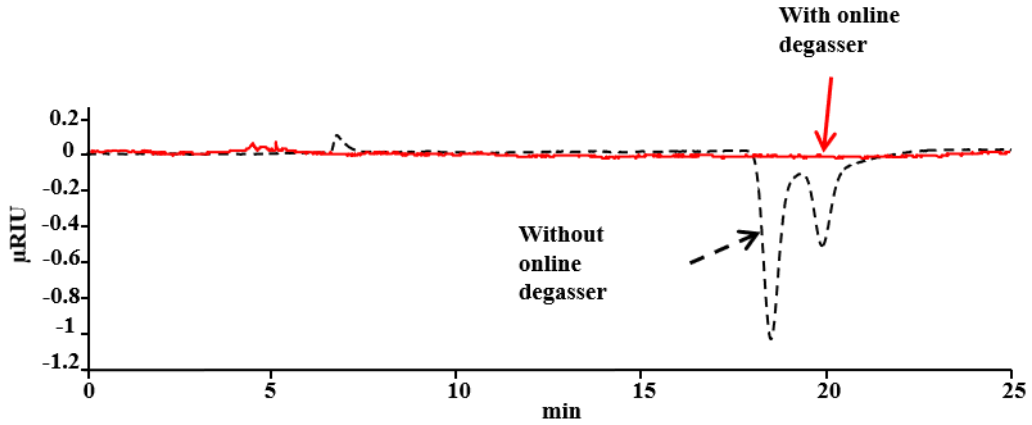

Fig. S1. Comparison of chromatograms with and without online degasser

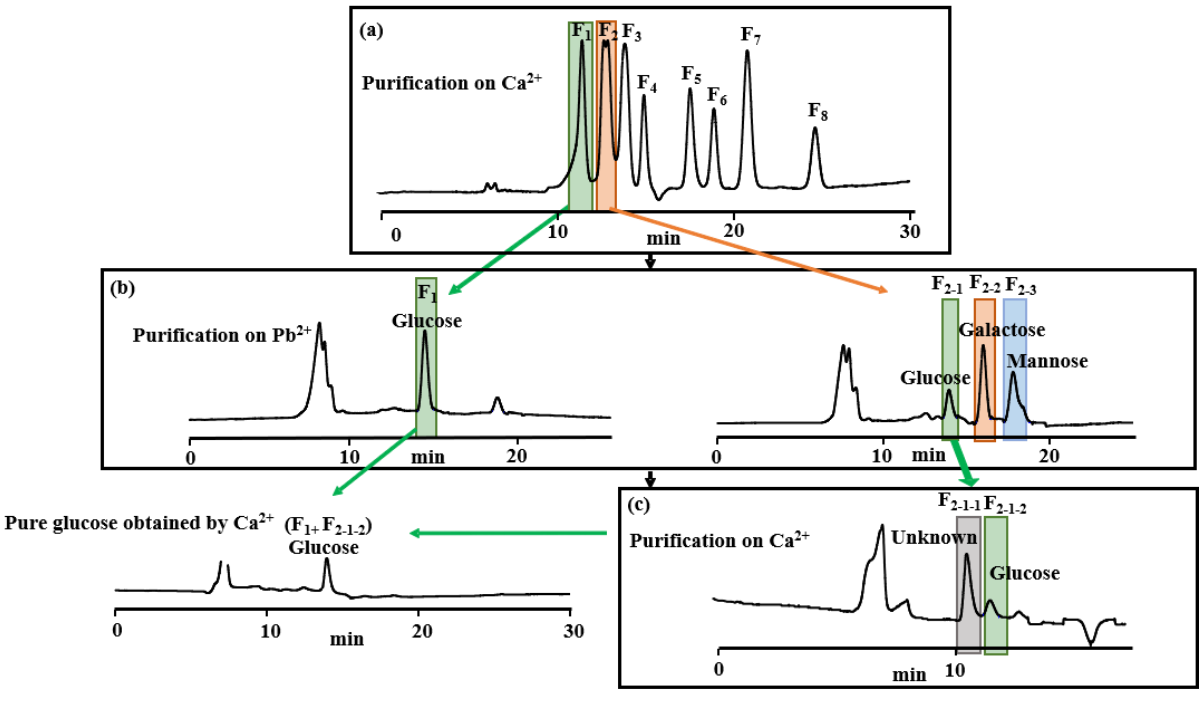

Fig. S2: Example of a standard monosaccharide mixture (50 µM each) purification on (a) Ca^{2+} column: F_1 (glucose)/F_2 (galactose + mannose)/F_3 (fructose + arabinose)/F_4 (galactosan)F_5 (mannitol)/F_6 (levoglucosan)/F_7 (sorbitol + xylitol)/F_8 (mannosan),

followed by purification on (b) Pb^{2+} column of F_1 and F_2 fractions: F_1 + $F_{2\text{-}1}$ (glucose)/$F_{2\text{-}2}$ (galactose)/$F_{2\text{-}3}$ (mannose) and (c) Ca^{2+} column of $F_{2\text{-}1}$ fraction : $F_{2\text{-}1\text{-}1}$ (unknown)/$F_{2\text{-}1\text{-}2}$ (glucose). Colored boxes correspond to peak(s) collection.

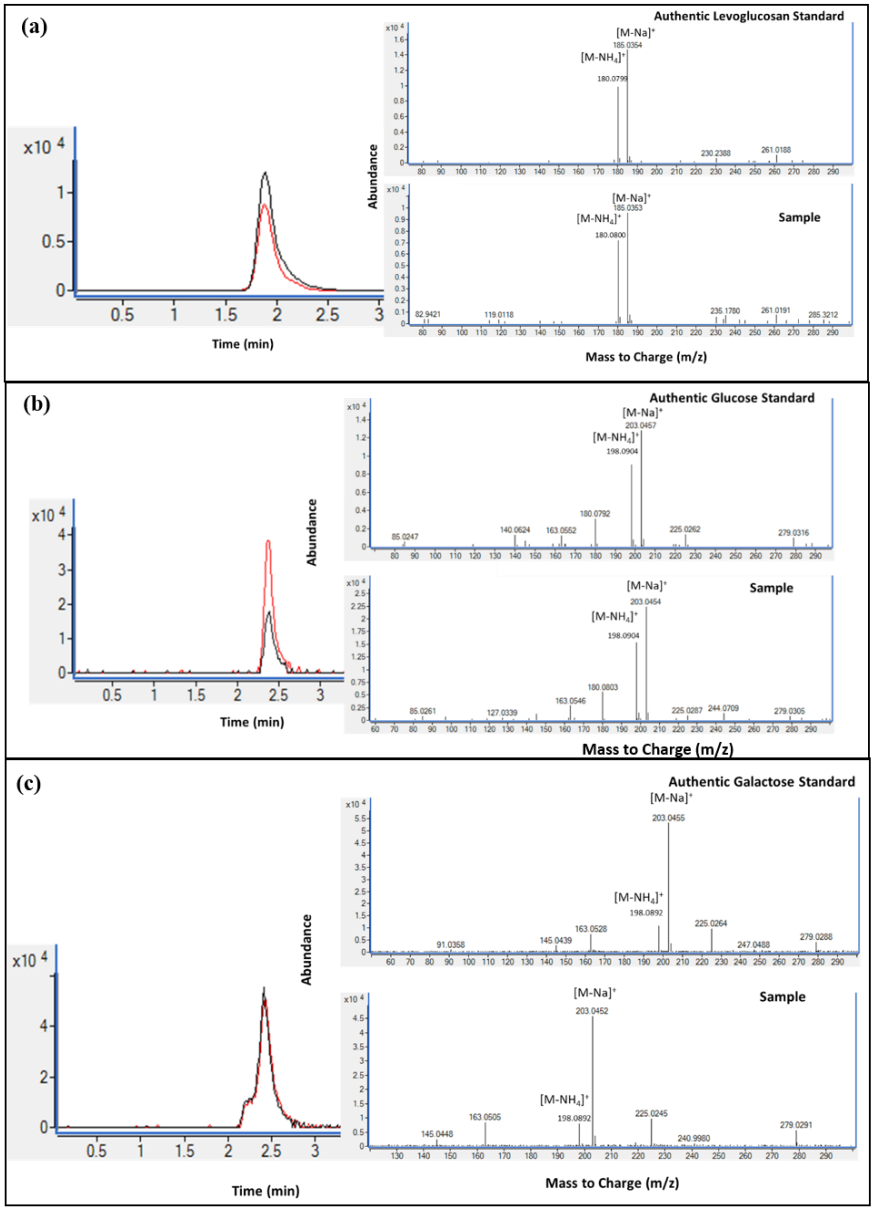

Fig. S3. Extracted ion chromatograms corresponding to the analysis of underivatized levoglucosan (a), glucose (b) and galactose (c). The black line corresponds to the respective authentic standard (~ 5ppm final concentration) and red line to the sample. In

all spectra, the molecular ion was detected as a Na^+ and NH_4^+ additive. More details are given in Table S3.

Table S1: Columns characteristics and analysis conditions used for the HPLC-RI system.

Column	RNO-Oligosaccharide	RCM-Monosaccharide	RPM-Monosaccharide
The ionic form	Na^+	Ca^{2+}	Pb^{2+}
Column size	200 × 10 mm	300 × 7.8 mm	300 × 7.8 mm
Stationary phase	Sulfonated styrene-divinylbenzene		
Cross linking	4%	8%	8%
Particles size	12 µm	9 µm	8 µm
Temperature	85 °C	85 °C	75 °C
Mobile phase	Degassed ultra-pure water		
Flow rate	0.3 mL min^{-1}	0.6 mL min^{-1}	0.6 mL min^{-1}
Run time	50 min	30 min	45 min

1046 **Table S2**. Monosaccharide purification yields after three sequential purifications
1047 (Ca^{2+}→ Pb^{2+} → Ca^{2+}) of a standard monosaccharide mixture (see text) at 50 µM (*n* = 3).

Standard	**Average yield**
	Mean ± Stdev
Glucose	36.32 ± 0.02
Galactose	29.28 ± 0.03
Mannose	25.17 ± 0.01
Fructose	20.44 ± 0.01
Arabinose	12.38 ± 0.01
Galactosan	15.22 ± 0.00
Mannitol	31.01 ± 0.01
Levoglucosan	31.49 ± 0.01
Xylitol	25.84 ± 0.01
Sorbitol	30.09 ± 0.03
Mannosan	32.21 ± 0.00

1048

1049

1050

1051 **Table S3**. Theoretical and measured masses (LC-Q-TOF-MS analysis) recorded as Na^+
1052 and NH_4^+ additives for levoglucosan, glucose and galactose.

	Theoretical mass		**Measured authentic standard mass**		**Measured purified compound mass**	
	Na^+	**NH_4^+**	**Na^+**	**NH_4^+**	**Na^+**	**NH_4^+**

	additive	additive	additive	additive	additive	additive
Levoglucosan (TSP)	185.0431	180.0877	185.0354	180.0799	185.0363	180.0800
Glucose (POM)	203.0537	198.0978	203.0457	198.0904	203.0454	198.0904
Galactose (POM)	203.0537	199.0978	203.0455	198.0892	203.0452	198.0892

References

[1]X. Cheng, L. a Kaplan, Improved Analysis of Dissolved Carbohydrates in Stream Water with HPLC-PAD, Anal. Chem. 73 (2001) 458–461. doi:10.1021/ac001059r.